


 Cite this: *RSC Adv.*, 2020, **10**, 26102

# A comparative study on the interface tension and interface dilational rheological properties of three sodium *N*-acyl aromatic amino acid surfactants

 Fan Zhang,<sup>a</sup> Qun Zhang,<sup>a</sup> Jian Yang,<sup>b</sup> Yawen Zhou,<sup>b</sup> \*<sup>b</sup> Zhaohui Zhou<sup>a</sup> and Ce Wang<sup>b</sup> 

Interface dilational rheology is useful for understanding and exploring the role of interface phenomena. However, relatively few studies have been conducted on the interface dilational rheological properties of *N*-acyl aromatic amino acid surfactants. Herein, surface tension and the dynamic interface tension and dilational rheological properties of three surfactants, namely, sodium *N*-lauroyl phenylalaninate (SLP), sodium *N*-lauroyl tyrosinate (SLTy), and sodium *N*-lauroyl citrate (SLTr) were investigated. The results show that the order of critical micelle concentration, which includes the surface tension at the critical micelle concentration, minimum area per surfactant molecule, and interfacial tension, was SLTr < SLTy < SLP. At a low surfactant concentration, the three surfactants exhibited a low-viscosity interfacial elastic film at the *n*-decane/water interface. The dilational modulus increased and the phase angle decreased with increase in frequency. However, the order of the dilational modulus was SLP < SLTy < SLTr, while the order of the phase angle change was SLTr < SLTy < SLP at the same frequency. With increase in surfactant concentration, the dilational modulus of SLP and SLTy increased and then decreased after a maximum value; however, the dilational modulus plot of SLTr demonstrated two maxima.

 Received 25th April 2020  
 Accepted 23rd June 2020

DOI: 10.1039/d0ra03713c

[rsc.li/rsc-advances](http://rsc.li/rsc-advances)

## 1. Introduction

Interface dilational rheology is a crucial research method for obtaining information on molecular arrangements at interfaces during intermolecular interactions and in supramolecular aggregates.<sup>1–3</sup> This method is useful for understanding and exploring the role of interface phenomena. Relevant research has become a hot spot in the field.<sup>4–9</sup> Practical application has confirmed that interface dilational rheology is simple and powerful and it has been extensively used in molecular surface interface interactions and their aggregates.<sup>10–13</sup>

Current research on the phenomenon of interface rheology mostly focuses on surfactant solution systems in which the rheological properties are affected by the hydrophobic alkyl chain length. For example, Li *et al.* investigated the dynamic dilational viscoelastic properties of *N*-2-(phenoxy)-tetradecanolytaurinate (12+B-T) and *N*-2-(4-ethylphenoxy)-tetradecanolytaurinate (12+2B-T), as well as the influence of time, dilational frequency, and molar concentration on the dilational modulus. Furthermore, phase angles at the air/water surface were investigated. The adsorption film was primarily elastic at low concentrations and exhibited viscoelastic

properties at high concentrations.<sup>14</sup> Li *et al.* investigated the dilational rheological properties of sodium trisubstituted linear alkylbenzene sulfonate and examined the effect of alkyl substitution on the molecular interface behavior at different positions of the benzene ring. The interface dilational elastic modulus increased with decrease in sulfonate *ortho*-chain length, whereas the dilational viscous modulus did not considerably change. The interface dilational elastic modulus and viscous modulus significantly increased with an increase in the sulfonate *meta*- and *para*-double chains.<sup>15</sup> However, the influence of the group near the hydrophilic group on the interface dilatational rheology is rarely reported.

Amino acid surfactants are environmentally friendly, mild, biodegradable, and have low toxicities. They can be applied to household chemicals,<sup>16</sup> food, biomedicine,<sup>17</sup> agriculture, and other industrial fields. Current research mostly focuses on *N*-acyl amino acid surfactants such as alanine, glycine, sarcosine, lysine, and glutamic acid.<sup>18–21</sup> Previous studies primarily focused on the synthesis<sup>22</sup> and basic properties, including the surface,<sup>23–26</sup> foam,<sup>27</sup> and gel properties,<sup>28</sup> of the surfactants. For example, Takassi *et al.* studied the critical micelle concentration of *N*-acyl lysine surfactants on the basis of conductivity, pH, and IFT.<sup>29</sup> However, few studies have been conducted on aromatic amino acid surfactants, especially regarding the interface dilational rheological properties of *N*-acyl aromatic amino acid surfactants.

<sup>a</sup>State Key Laboratory of Enhanced Oil Recovery, Research Institute of Petroleum Exploration & Development, Beijing 100083, PR China

<sup>b</sup>Beijing Technology and Business University, Beijing 100048, PR China. E-mail: zhouyw@th.btbu.edu.cn



In this study, three *N*-acyl aromatic amino acid surfactants (sodium *N*-lauroyl phenylalaninate [SLP], sodium *N*-lauroyl tyrosinate [SLTy], and sodium *N*-lauroyl citrate [SLTr]) were studied. The surface tension, dynamic interface tension, and interface dilational rheological properties of these three *N*-acyl aromatic amino acid surfactants at the *n*-decane/water interface were then investigated. The influence of the molecular structure on the interface dilational rheological properties of *N*-acyl aromatic amino acid surfactants is discussed.

## 2. Experimental

### 2.1. Materials

SLP, SLTy, and SLTr were synthesized in our laboratory at a purity of >97%. The chemical structures are shown in Scheme 1. *n*-Decane (analytical reagent) was purchased from Shanghai Aladdin Biochemical Technology Co., Ltd. (China), and the solutions were prepared using ultrapure water.

### 2.2. Surface tension measurements

The surface tension was measured using the Wilhelmy plate method with a surface tension meter (DCAT21, DataPhysics, Germany) at  $25.0 \pm 0.1$  °C. The standard deviation was set to  $\pm 0.02$  mN m<sup>-1</sup> and the average value was measured three times to obtain the surface tension value ( $\gamma$ ) corresponding to the concentration (*c*) of sodium *N*-lauryl amino acid. The  $\gamma$ -lg *c* curve was plotted to obtain the surface tension diagram. The cmc and the surface tension value at the cmc ( $\gamma_{\text{cmc}}$ ) were also obtained. The corresponding maximum excess surface concentration ( $\Gamma_{\text{max}}$ ), minimum area per surfactant molecule

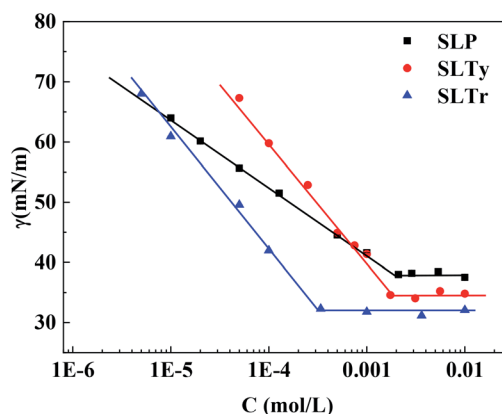


Fig. 1 Surface tension of *N*-acyl aromatic amino acid surfactants.

( $A_{\text{min}}$ ), standard free energy ( $\Delta G_{\text{m}}^{\theta}$ ), and surface adsorption efficiency ( $\text{pC}_{20}$ ) were obtained as per formulae (1)–(4).

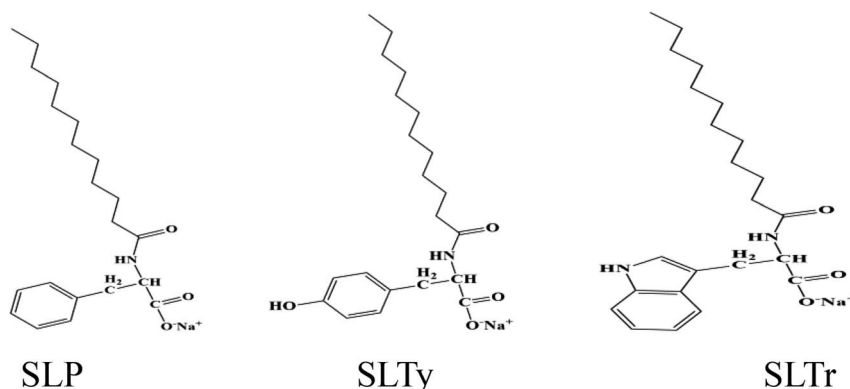
$$\Gamma_{\text{max}} = -\frac{1}{2.303nRT} \frac{d\gamma}{d \lg C} \quad (1)$$

$$A_{\text{min}} = \frac{1}{N_{\text{A}}\Gamma_{\text{max}}} \quad (2)$$

$$\text{pC}_{20} = -\lg C_{20} \quad (3)$$

$$\Delta G_{\text{m}}^{\theta} = nRT \ln \text{cmc} \quad (4)$$

where *R* is the molar gas constant 8.314 J mol<sup>-1</sup> K<sup>-1</sup>, the unit of temperature is K, the  $\gamma$  unit is mN m<sup>-1</sup>, the  $\Gamma_{\text{max}}$  unit is mol m<sup>-2</sup>, *n* = 2, *N<sub>A</sub>* is Avogadro constant ( $6.023 \times 10^{23}$ ).



Scheme 1 Chemical structures of SLP, SLTy, and SLTr.

Table 1 Surface parameters of *N*-acyl aromatic amino acid surfactants

SAA	Cmc (mmol L <sup>-1</sup> )	$\gamma_{\text{cmc}}$ (mN m <sup>-1</sup> )	$\Gamma_{\text{max}}$ ( $\times 10^{-6}$ ) (mol m <sup>-2</sup> )	$A_{\text{min}}$ ( $\times 10^{-14}$ ) (m <sup>2</sup> )	pC <sub>20</sub>	$\Delta G_{\text{m}}^{\theta}$ (kJ mol <sup>-1</sup> )
SLP	2.02	37.73	0.99	1.68	3.97	-30.74
SLTy	1.74	34.59	1.74	0.95	3.62	-31.48
SLTr	0.34	32.36	1.77	0.94	4.48	-39.62



### 2.3. Dynamic interface tension and interface dilational rheological measurements

**2.3.1. Experimental.** The properties of the interface dilational rheology were measured using an oscillating drop tension meter (OCA20, DataPhysics, Germany). The main components of the device included a light source, a CCD

camera, an oscillator, and a needle tube for forming liquid droplets. The aqueous phase droplet in the needle tube was injected into *n*-decane, and the droplet was suspended on the needle to form an oil–water interface. Then, the droplet was subjected to oscillation at a frequency of 0.1 Hz. The camera captured a real-time image of the droplet area. Through the corresponding software processing, the changes in the dynamic

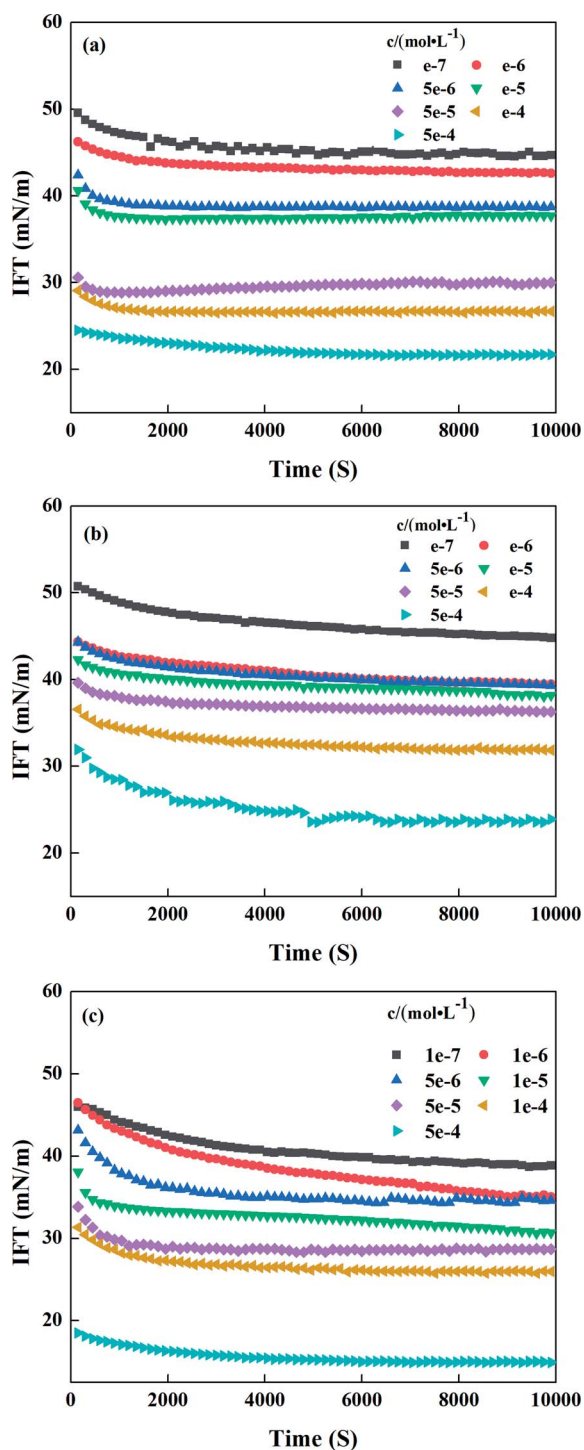


Fig. 2 Dynamic interface tension of sodium *N*-acyl aromatic amino acid surfactants at different concentrations: (a) SLP (b) SLTy, and (c) SLTr.

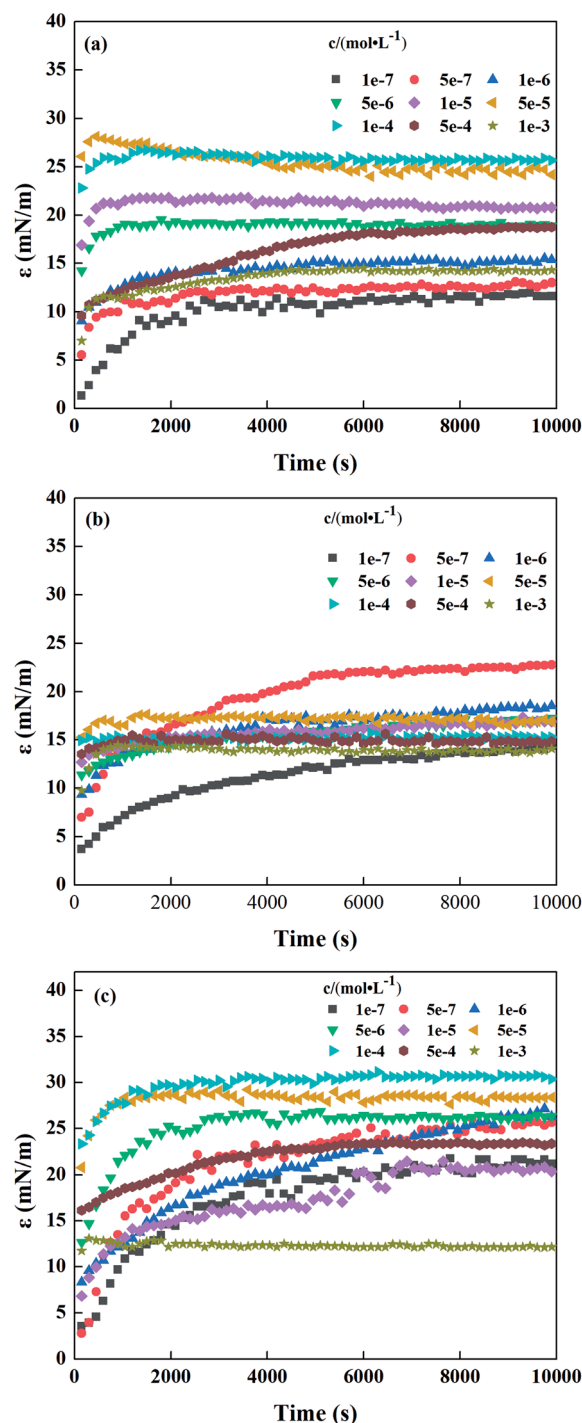


Fig. 3 Interface dilational modulus of sodium *N*-acyl aromatic amino acid surfactant (a) SLP, (b) SLTy, and (c) SLTr.



interfacial tension and dynamic dilational parameters of the adsorption process were obtained until the interfacial tension reached equilibrium. Then, the dilational modulus and phase angle were measured at oscillation frequencies between 0.005 and 0.1 Hz. The experiment was carried out when the area of the droplets ( $A$ ) that expanded to  $\Delta A/A$  was 20%. The water phase was a *N*-lauryl amino acid sodium surfactant solution and the experiments were performed with solutions of different concentrations.

**2.3.2. Relevant theory.** When the interface is compressed and periodically expanded, the interfacial tension periodically changes. The dilational modulus is defined as the change in interface tension that occurs with a small relative change in the interface area,<sup>30</sup> which is described as follows:

$$\varepsilon = \frac{d\gamma}{d \ln A} \quad (5)$$

where  $\varepsilon$  is the dilational modulus,  $\gamma$  is the interface tension, and  $A$  is the interface area.

The phase angle ( $\theta$ ) of dilational modulus is a certain phase difference  $\theta$  between the periodic variation of the interface tension and the periodic variation of the interface area for the viscoelastic interface. Therefore, the dilational modulus can be expressed as a complex quantity:

$$\varepsilon = \varepsilon_d + i\omega\eta_d \quad (6)$$

where  $\varepsilon_d$  is the dilational elasticity,  $\eta_d$  is the dilational viscosity, and  $\omega$  is the frequency at which the interface area sinusoidally changes. The real part  $\varepsilon_d$  and the imaginary part  $\omega\eta_d$  are referred to as the storage modulus and loss modulus, respectively, and reflect the contributions of the elastic and viscous portions of the viscoelastic interface. The formulae for dilational elasticity and dilational viscosity are as follows:

$$\varepsilon_d = |\varepsilon| \cos \theta \quad (7)$$

$$\eta_d = (|\varepsilon|/\omega) \sin \theta \quad (8)$$

### 3. Results and discussion

#### 3.1. Surface activity of sodium *N*-acyl aromatic amino acid surfactants

The surface tensions of SLP, SLTy, and SLTr at different concentrations were measured at 25 °C. The results are shown in Fig. 1 and indicate that the surface tension of the three surfactants showed obvious folding points with changes in concentration, thus reducing the surface tension to 30–40 mN

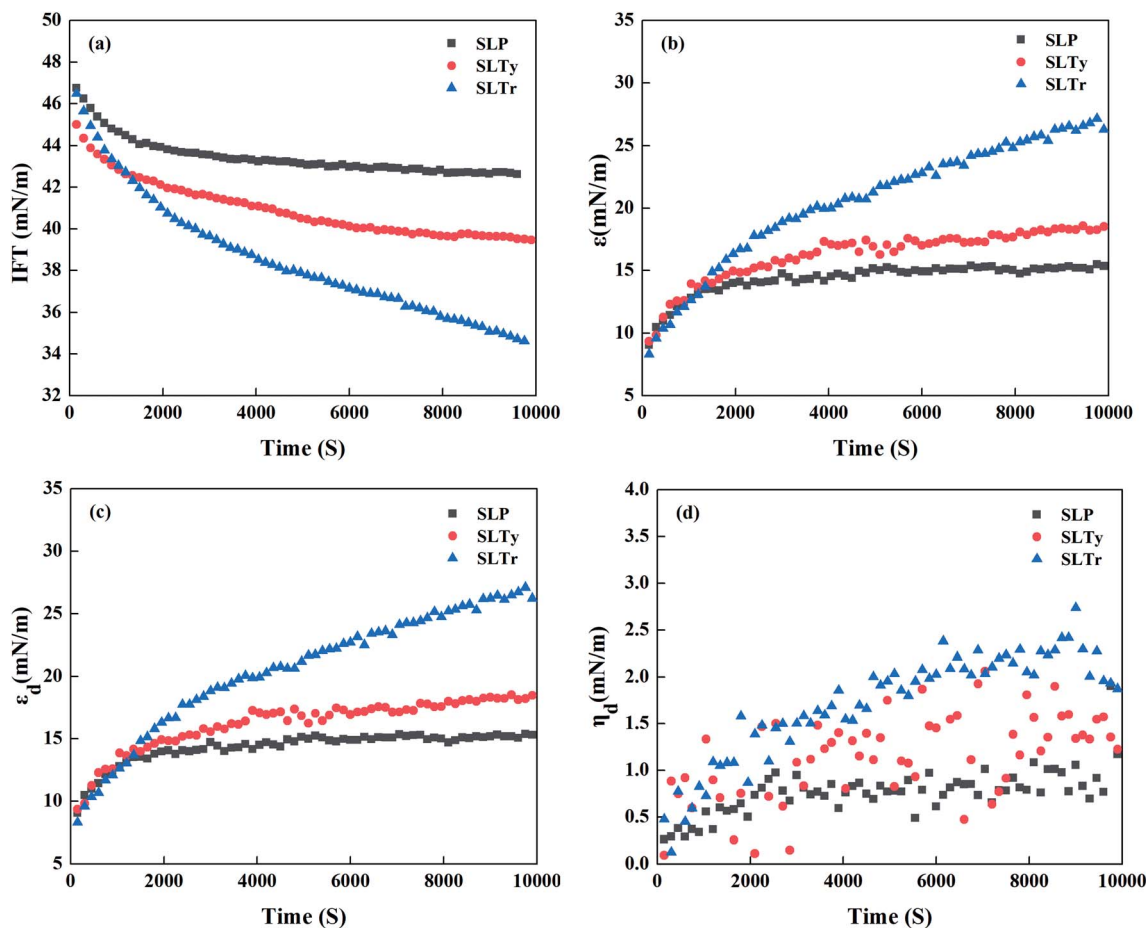


Fig. 4 Dynamic interfacial tension and dynamic dilational rheological properties of sodium *N*-acyl aromatic amino acid surfactants: (a) interfacial tension, (b) dilational modulus, (c) dilational elasticity, and (d) dilational viscosity.



$\text{m}^{-1}$ . The surface activity parameters of SLP, SLTy, and SLTr are then shown in Table 1, where the cmc of SLP, SLTy, and SLTr are presented as  $2.02 \times 10^{-3}$ ,  $1.74 \times 10^{-3}$ , and  $0.34 \times 10^{-3} \text{ mol L}^{-1}$  respectively, and the  $\gamma_{\text{cmc}}$  values were calculated as 37.73, 34.59, and  $32.36 \text{ mN m}^{-1}$ , respectively. The order of cmc and  $\gamma_{\text{cmc}}$  is  $\text{SLTr} < \text{SLTy} < \text{SLP}$ . The surface parameters,  $\Gamma_{\text{max}}$  and  $A_{\text{min}}$ , in Table 1 indicate the same order and SLTr had the largest  $\Gamma_{\text{max}}$  and the smallest  $A_{\text{min}}$ .  $\text{pC}_{20}$  reflects the efficiency of reducing surface tension. Table 1 shows that SLTr had the highest efficiency for reducing surface tension. The  $\Delta G_{\text{m}}^{\theta}$  values of the three surfactants were negative and the  $\Delta G_{\text{m}}^{\theta}$  value of SLTr was the largest, which indicates that the micelles spontaneously formed and SLTr was most likely to form micelles.

### 3.2. Dynamic interface tension and dynamic dilational rheology properties of sodium *N*-acyl aromatic amino acid surfactants

The dynamic interface tensions of sodium *N*-acyl amino acid surfactant solutions at different concentrations are shown in Fig. 2. Fig. 2(a)–(c) show that the equilibrium interface tension of the three surfactants decreased with increasing concentration. However, at the same concentration, the three surfactants had evidently different effects on the reduction of the interface tension. The order of dynamic interface tension was  $\text{SLTr} < \text{SLTy} < \text{SLP}$  when the concentration was  $1 \times 10^{-6} \text{ mol L}^{-1}$ . This may be due to the presence of phenolic hydroxyl groups in the SLTy molecules and indole groups in the SLTr molecules, which enhance the intermolecular interactions, thereby resulting in a closer intermolecular interaction between SLTy and SLTr surfactant molecules. Consequently, the adsorption at the interface is more effective, thereby improving the ability to reduce the interfacial tension, which is consistent with the measured surface tension results.

Fig. 3 shows the interface dilational modulus trend of the three surfactant solutions at different concentrations with increasing time. Less time was required to reach dilational modulus equilibrium as the surfactant concentration increased. However, the dilational modulus did not show a monotonic trend with increase in concentration, which may be attributed to the dual action of molecular diffusion and interface molecular interactions of the interface adsorption process.

The changes in the dynamic interface tension, dilational modulus, dilational elasticity, and dilational viscosity as a function of time for the three sodium *N*-acyl amino acid surfactants at the concentration of  $1 \times 10^{-6} \text{ mol L}^{-1}$  are depicted in Fig. 4(a)–(d). It is observed that the equilibrium time of the dynamic interface tension of the three surfactants was different in Fig. 4(a). The interface tension reached equilibrium after 2000 and 6000 s for SLP and SLTy, respectively, but the interface tension of SLTr did not reach equilibrium until 10 000 s. From Fig. 4(b) and (c), we can see that the dilational modulus and dilational elastic modulus of SLTy and SLP gradually increased with time until equilibrium was reached and the time required to reach equilibrium was almost the same as the time required to reach the interface tension equilibrium. However, the dilational modulus and dilational elastic modulus of SLTr continued to increase during the investigated

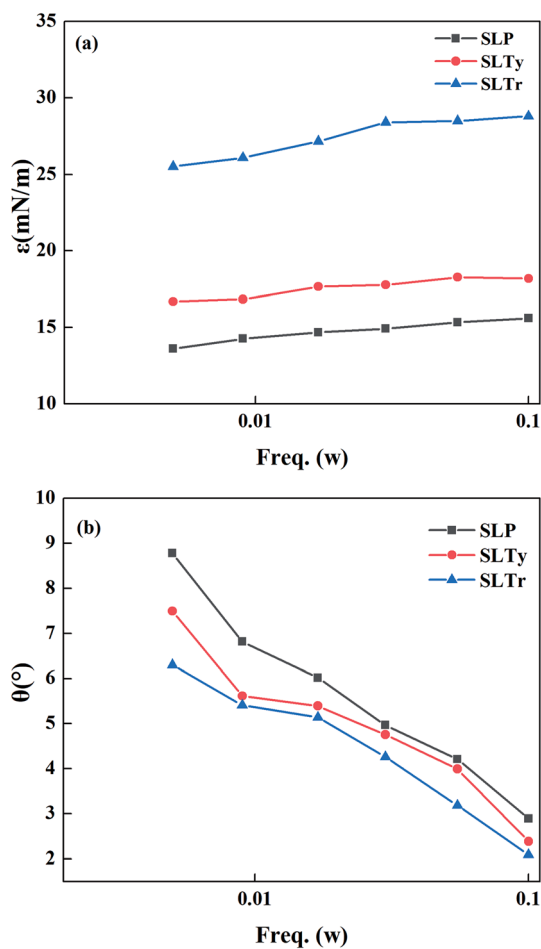


Fig. 5 Interface dilational modulus (a) and phase angle (b) of sodium *N*-acyl aromatic amino acid surfactants as a function of working frequency.

timeframe. In Fig. 4(d), we can see that the dilational viscous modulus of the three surfactants did not considerably change and the viscosity was  $< 3 \text{ mN m}^{-1}$ , thereby indicating that the interface was elastic with a minor contribution from viscosity.

### 3.3. Effect of working frequency on the interface dilational properties of sodium *N*-acyl aromatic amino acid surfactant

Working frequency is an important factor that affects the dilational rheological parameters. Therefore, we examined the effect of working frequency on the interface dilational rheological properties of the three sodium *N*-acyl aromatic amino acid surfactants. Fig. 5 shows the changes in the interface dilational modulus (a) and phase angle (b) of the three surfactants with working frequency at the concentration of  $1 \times 10^{-6} \text{ mol L}^{-1}$ . As can be seen in Fig. 5(a), the dilational modulus of the three surfactants tended to increase with increase in frequency. This may be a result of the available time, which was sufficient to eliminate the interfacial tension gradient generated by interfacial deformation through the diffusion exchange when the surfactant molecules were at low frequencies, thus resulting in a small dilational modulus. As the working frequency increased, the interface area rapidly changed and there was insufficient time to eliminate



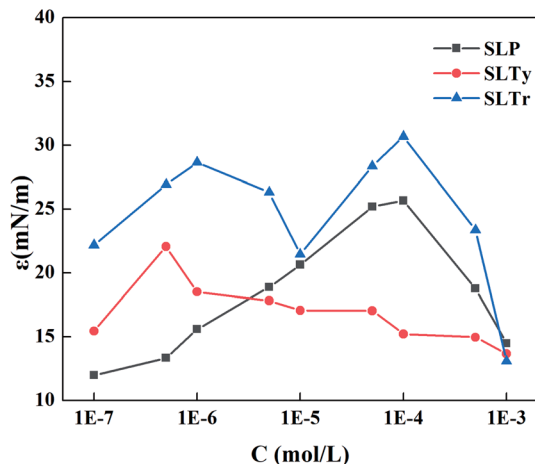


Fig. 6 Interface dilational modulus of *N*-acyl aromatic amino acid surfactants as a function of concentration.

the interface tension gradient; thus, the dilational modulus was larger. Therefore, the dilational modulus increased with increase in frequency. At the same frequency, the order of dilational modulus was  $SLP < SLTy < SLTr$ . This was due to the stronger intermolecular interactions in SLTy and SLTr by the phenolic hydroxyl and indole groups. From Fig. 5(b), we can see that the phase angles of the three surfactants decreased as the working frequency increased. This was because there was less time for the disturbed interfacial adsorption layer to restore the equilibrium by relaxation processes such as diffusion exchange with increase in working frequency. The time required for the diffusion exchange relaxation process to occur was shorter and had a minimal contribution. Thus, it slightly contributed to the viscous modulus and resulted in a gradual decrease in the phase angle. At the same frequency, the phase angle of SLTr was the smallest, as shown in Fig. 4(c) and (d). At 0.1 Hz, the elastic modulus and viscous modulus of SLTr were the largest among the three surfactants but the viscous modulus accounted for the smallest proportion. Therefore, the phase angle of SLTr was the smallest.

#### 3.4. Effect of surfactant concentration on the interface dilational rheological properties

Fig. 6 shows the tendency of interface dilational modulus of three sodium *N*-acyl aromatic amino acid surfactants at

a working frequency of 0.1 Hz. For SLP and SLTy, the interface dilational modulus increased and then decreased as the surfactant concentration increased, and the maximum values appeared when the surfactant concentration was  $1 \times 10^{-4}$  and  $5 \times 10^{-7}$  mol L<sup>-1</sup>, respectively. The interface dilational modulus was closely related to surfactant concentration. The increase in surfactant concentration had two effects on the interface dilational modulus. First, the surfactant concentration on the interface increased with increasing bulk phase concentration of the surfactant molecules, which strengthened the interface molecular interactions and increased the dilational modulus of the interface film. Secondly, the molecular exchange between the bulk solution and the interface increased with increasing surfactant concentration, which restored the equilibrium of the interface and reduced the interface dilational modulus. The combination of these two factors led to a maximum dilational modulus with increasing surfactant concentration.<sup>15</sup>

Note that with increase in concentration, two dilational modulus maxima were observed for SLTr, *i.e.*, a maximum dilational modulus was observed in the concentration range from  $1 \times 10^{-7}$  to  $1 \times 10^{-5}$  mol L<sup>-1</sup>, and another maximum value was observed in the concentration range from  $1 \times 10^{-5}$  to  $1 \times 10^{-3}$  mol L<sup>-1</sup>. When the SLTr concentration increased to the range from  $1 \times 10^{-7}$  to  $1 \times 10^{-5}$  mol L<sup>-1</sup>, more SLTr molecules were adsorbed on the interface, which caused interactions between the surfactant molecules and therefore the dilational modulus increased. Then, the diffusion exchange between the interface and bulk molecules increased with increase in SLTr concentration, which helped the interactions to restore equilibrium and decreased dilational modulus; thus, the first maximum appeared. When the SLTr concentration increased to the range from  $1 \times 10^{-5}$  to  $1 \times 10^{-3}$  mol L<sup>-1</sup>, the indole groups overlapped, as shown in Fig. 7(a). The interactions between the molecules enhanced and the dilational modulus increased by hyperconjugation. Then, with increase in surfactant concentration, the arrangement of the SLTr molecules on the interface tightened, which changed the orientation of indole group and destroyed hyperconjugation. As shown in Fig. 7(b), the diffusion exchange between the bulk phase and the interface was enhanced, resulting in a reduction in the dilational modulus. Therefore, the interface dilational modulus passed *via* the second maximum.<sup>31</sup> The appearance of two maxima was observed in other studies. For example, with

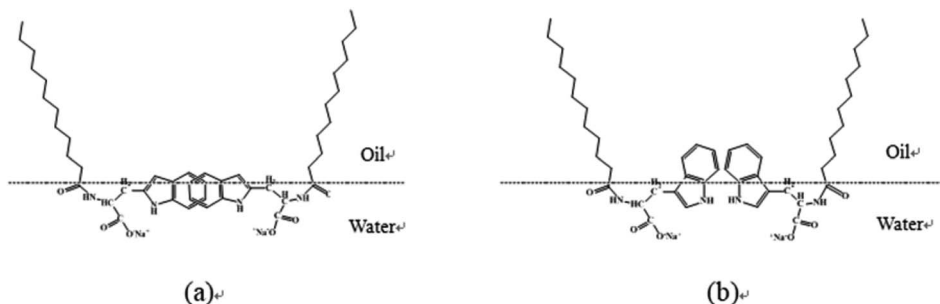


Fig. 7 Schematic of SLTr on the interface adsorption layer.



increase in concentration, the dilational modulus of sodium lauryl glycolglycine had two maxima, and the second maximum appeared because of enhanced hydrogen bonding as the distance between molecules shortened.<sup>32</sup> Feng *et al.* reported that, for the gemini surfactant of oligooxa- $\alpha,\omega$ -bis(*m*-octylbenzene sulfonate) with eight ethylene oxide groups (C<sub>8</sub>E<sub>8</sub>C<sub>8</sub>), the dilational modulus displayed two maxima with increasing concentration, which were attributed to the circular conformation of the spacer chain entering the water side of the interface and the rearrangement and orientation of the molecules in the interface layer.<sup>33</sup>

## 4. Conclusion

In summary, we studied the surface tension and dilational rheological properties at the *n*-decane/water interface of SLP, SLTy, and SLTr with aromatic ring structures. The results showed that the presence of the phenolic hydroxyl groups in SLTy and the indolyl groups in SLTr enhanced the intermolecular interactions, which enabled the surfactant molecules to adsorb more on the surface or interface and arrange more tightly, thus resulting in lower cmc,  $\gamma_{\text{cmc}}$ , and interface tension for SLTy and SLTr. The interface dilational modulus of the three surfactants increased and the phase angle decreased with increase in frequency. First, the dilational modulus of SLP and SLTy increased and then decreased with increase in surfactant concentration. The structure of the indole ring of the SLTr molecule had an important influence on the interface rheological behavior and the dilational modulus showed two maxima when plotted against increasing surfactant concentration.

## Conflicts of interest

The authors declare that they have no conflict of interest.

## Acknowledgements

This work was financially supported by the National Key R&D Program of China (No. 2017YFB0308700).

## References

- 1 L. Yue, Z. He, Y. Wang, Y. Shang and H. Liu, *Acta Phys.-Chim. Sin.*, 2014, **30**, 2291–2299.
- 2 A. Akanno, E. Guzmán, L. Fernández-Peña, F. Ortega and R. G. Rubio, *Molecules*, 2019, **24**, 3442.
- 3 H. Fang, L. Wang, H. Zong, L. Mao and L. Zhang, *Acta Pet. Sin.*, 2011, **27**, 746–752.
- 4 C. Wang, X. Cao, Y. Zhu, Z. Xu, Q. Gong, L. Zhang, L. Zhang and S. Zhao, *Soft Matter*, 2017, **13**, 8636–8643.
- 5 W. Situ, H. Lu, C. Ruan, L. Zhang, Y. Zhu and L. Zhang, *Colloids Surf., A*, 2017, **533**, 231–240.
- 6 C. Wang, L. Zhao, B. Xu, X. Cao, L. Guo, L. Zhang, L. Zhang and S. Zhao, *Colloids Surf., A*, 2018, **541**, 78–86.
- 7 Q. Zhu, C. Wang, N. Khalid, S. Qiu and L. Yin, *Food Hydrocolloids*, 2017, **73**, 194–202.
- 8 D. Wang, L. Luo, L. Zhang, S. Zhao, L. Wang, Q. Gong, L. Liao, Y. Chu and J. Yu, *J. Dispersion Sci. Technol.*, 2007, **28**, 725–736.
- 9 W. Kloek, T. V. Vliet and M. Meinders, *J. Colloid Interface Sci.*, 2001, **237**, 158–166.
- 10 Y. Zhu, X. Song, L. Luo, L. Zhang, S. Zhao and J. Yu, *Chem. Res. Chin. Univ.*, 2010, **31**, 2445–2452.
- 11 Q. Zhang, Z. Zhou, L. Dong, H. Wang, H. Cai, F. Zhang, L. Zhang, L. Zhang and S. Zhao, *Colloids Surf., A*, 2014, **455**, 97–103.
- 12 E. Guzmán, L. Fernández-Peña, A. Akanno, S. Llamas, F. Ortega and R. G. Rubio, *Coatings*, 2019, **9**, 438.
- 13 Y. Zhu and G. Xu, *Acta Phys.-Chim. Sin.*, 2009, **25**, 191–200.
- 14 Z. Li, L. Zhang, F. Yan, L. Zhang, S. Zhao and J. Yu, *Acta Phys.-Chim. Sin.*, 2009, **25**, 1939–1944.
- 15 L. Zhang, X. Wang, Q. Gong, L. Zhang, L. Zhang, S. Zhao, J. Yu and J. Yu, *J. Colloid Interface Sci.*, 2008, **327**, 451–458.
- 16 Y. Wei, H. Zhu, H. Li and Q. Li, *Deterg. Cosmet.*, 2003, **26**, 20–23.
- 17 S. Ghosh and J. Dey, *J. Colloid Interface Sci.*, 2015, **458**, 284–292.
- 18 S. Roy and J. Dey, *Langmuir*, 2005, **21**, 10362–10369.
- 19 A. Colomer, A. Pinazo, M. A. Manresa, M. P. Vinardell, M. Mitjans, M. R. Infante and L. Perez, *J. Med. Chem.*, 2011, **54**, 989–1002.
- 20 A. Colomer, A. Pinazo, M. T. Garcia, M. Mitjans, M. P. Vinardell, M. R. Infante, V. Martinez and L. Perez, *Langmuir*, 2012, **28**, 5900–5912.
- 21 Y. Zhang, M. Jin, R. Lu, Y. Song, L. Jiang, Y. Zhao and T. Li, *J. Phys. Chem. B*, 2002, **106**, 1960–1967.
- 22 R. Bordes and K. Holmberg, *Colloids Surf., A*, 2011, **391**, 32–41.
- 23 Y. Li, K. Holmberg and R. Bordes, *J. Colloid Interface Sci.*, 2013, **411**, 47–52.
- 24 A. Mohanty and J. Dey, *Langmuir*, 2004, **20**, 8452–8459.
- 25 T. Yoshimura, A. Sakato, K. Tsuchiya, T. Ohkubo, H. Sakai, M. Abe and K. Esumi, *J. Colloid Interface Sci.*, 2007, **308**, 466–473.
- 26 A. Ghosh and J. Dey, *J. Phys. Chem. B*, 2008, **112**, 6629–6635.
- 27 W. Qiao, Z. Zheng, H. Peng and L. Shi, *Tenside, Surfactants, Deterg.*, 2012, **49**, 161–166.
- 28 A. Ghosh and J. Dey, *Langmuir*, 2009, **25**, 8466–8472.
- 29 M. A. Takassi, A. Hashemi, A. Rostami and A. Zadehnazari, *Pet. Sci. Technol.*, 2016, **34**, 1521–1526.
- 30 L. Zhang, X. Wang, Q. Gong, L. Luo, L. Zhang, S. Zhao and J. Yu, *Acta Phys.-Chim. Sin.*, 2007, **23**, 1881–1885.
- 31 F. Yan, L. Zhang, R. Zhao, H. Huang, L. Dong, L. Zhang, S. Zhao and J. Yu, *Colloids Surf., A*, 2012, **396**, 317–327.
- 32 C. Wang, Z. Chen, J. Dong, S. Ullah, L. Zhao, G. Zhang and B. Xu, *Soft Matter*, 2019, **15**, 699–708.
- 33 J. Feng, X. Liu, L. Zhang, S. Zhao and J. Yu, *Langmuir*, 2010, **26**, 11907–11914.

